Optical OFDM With Single-Photon Avalanche Diode

Yichen Li, Majid Safari, Robert Henderson, and Harald Haas

***Abstract*— In this letter, an optical orthogonal frequency division multiplexing (OFDM) system based on a single-photon avalanche diode (SPAD) receiver is presented. SPAD detectors do not require a transimpedance amplifier as they operate in the Geiger mode. This poses challenges on detecting continuous data carrying signals. However, in this letter, we show that OFDM signals can indeed be detected, and the bit error ratio performances of both dc-biased optical OFDM and asymmetrically clipped optical OFDM are investigated. The investigations are carried out in the absence of background light. The results are compared with those of standard optical OFDM with convetional photodiode receivers. The SPAD-based OFDM system shows superior power efficiency over the state-of-the-art counterpart, and it can reach receiver sensitivities that are comparable with existing radio frequency systems.**

***Index Terms*— Visible light communication (VLC), Li-Fi, photon counting receiver, single-photon avalanche diode (SPAD).**

I. Introduction

CURRENT visible light communication (VLC) systems are mainly realized by high speed light emitting diodes (LEDs) as transmitters and photodiodes (PDs) as receivers. To date, a wireless VLC system using a single LED can achieve speeds greater than 3 Gb/s [1]. However, the incoherent light output of the LED means that information can only be encoded in the intensity level. As a consequence, only real-valued and positive signals can be used for data modulation. This is in contrast to radio frequency (RF) systems which make use of complex valued and bi-polar signals. Therefore, data modulation in VLC system is accomplished by using intensity modulation (IM) and direct detection (DD) system. On-off keying (OOK), pulse position modulation (PPM) and pulse amplitude modulation (PAM) are some of the common modulation schemes used in conjunction with IM/DD transmission [2].

For high-speed data transmission, orthogonal frequency division multiplexing (OFDM) is applied in order to get closer to the channel capacity by employing adaptive bit and power loading. Standard OFDM used in RF communications has to be adapted to realise IM/DD systems [3]. Optical OFDM (O-OFDM) needs to produce real-valued symbols. This can be achieved by imposing Hermitian symmetry on the information frame before the inverse fast Fourier transform (IFFT) operation during the signal generation phase. This comes at the expense of half of the spectral efficiency. Various O-OFDM modulation schemes have been realized in VLC such as DC-biased optical OFDM (DCO-OFDM), asymmetrically clipped optical OFDM (ACO-OFDM), unipolar OFDM (U-OFDM) and non-DC-biased OFDM (NDC-OFDM) [4]–[6].

In general, VLC systems make use of conventional PDs, such as positive-intrinsic-negative (PIN) diodes and avalanche photo diodes (APDs). However, for low power and long distance transmission, these PDs may not yield satisfactory performance results as the transimpedance amplifier (TIA) significantly reduces the sensitivity of the receiver. In this letter, single-photon avalanche diodes (SPADs) are considered as detector devices for O-OFDM systems. The SPAD detector does not require a TIA, and, thus, the output signal is not distorted by thermal noise in the same way as in PDs. This is one reason for the higher sensitivity of a SPAD detector. When the VLC system is applied in long distance transmission, such as in a gas well downhole monitoring system [7] and data transmission over plastic optical fibres (POF) [8], the number of photons reaching the receivers are typically significantly smaller than in short-distance communication links, and the signal is buried in noise. In these scenarios, and when compared with conventional PDs, a SPAD-based receiver is expected to be most suitable. A SPAD receiver can only detect one photon within a device specific dead time which constraints the ability to recover a signal. In addition, since the output of the detector is a photon count value, there is a maximum number of photons that the system can detect. This limits the maximum tolerable optical irradiance which results in a receiver clipping distortion. This letter investigates the performance of the SPAD-based OFDM system over long-distance optical links in the absence of background light.

The rest of this letter is organized as follows. The system model of the OFDM system with an SPAD array receiver is described in Section II. Section III reports results arising from the comparison with the PD-based OFDMs system followed by a discussion. Finally, Section IV concludes this letter.

II. Principles of OFDM With SPAD

A. Optical OFDM Modulation and Demodulation

Fig. 1 illustrates the system model of OFDM with SPAD receivers. The transmitter part is the same as in OFDM systems with PD receivers [9]. The input bit stream is transformed into complex symbols, $\mathbf{X}(n)$, by a M-QAM modulator, where M is the constellation size. The symbols are allocated on to N subcarriers, $\mathbf{X}(k)$, $k = 0, \cdots, N-1$.

Manuscript received October 30, 2014; revised January 21, 2015; accepted January 28, 2015. Date of publication February 10, 2015; date of current version April 6, 2015. This work was supported by the U.K. Engineering and Physical Sciences Research Council under Grant EP/K008757/1.

Y. Li, M. Safari, and H. Haas are with the Li-Fi Research and Development Centre, The University of Edinburgh, Edinburgh EH8 9YL, U.K. (e-mail: yichen.li@ed.ac.uk; majid.safari@ed.ac.uk; h.haas@ed.ac.uk).

R. Henderson is with the School of Engineering, Institute for Integrated Micro and Nano Systems, The University of Edinburgh, Edinburgh EH8 9YL, U.K. (e-mail: robert.henderson@ed.ac.uk).

Digital Object Identifier 10.1109/LPT.2015.2402151

1041-1135 © 2015 IEEE. Translations and content mining are permitted for academic research only. Personal use is also permitted, but republication/redistribution requires IEEE permission. See http://www.ieee.org/publications_standards/publications/rights/index.html for more information.

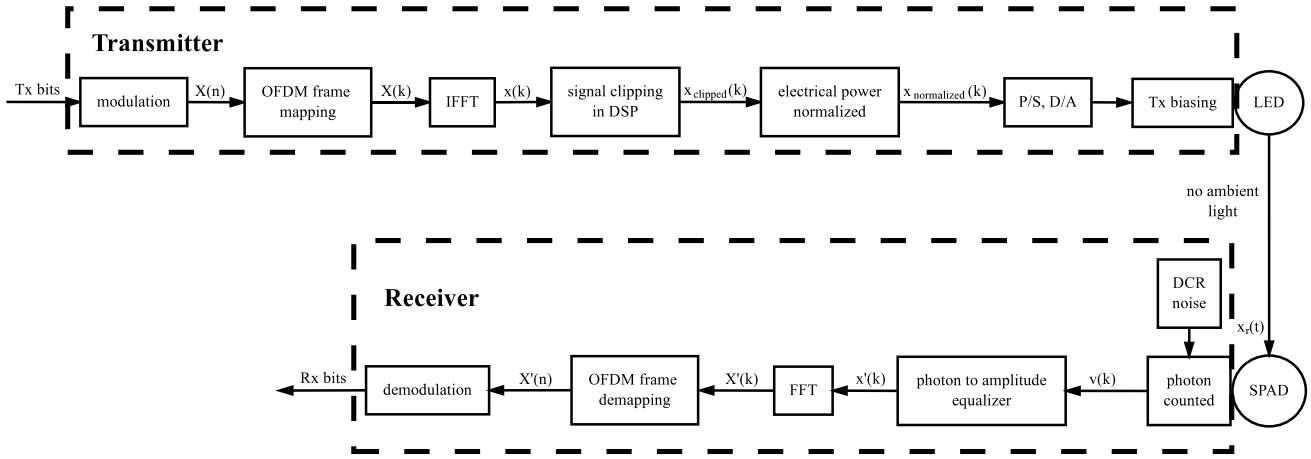

Fig. 1. Block diagram of the SPAD-based OFDM system.

In OFDM, N denotes the size of IFFT/FFT, where N is set to 2048 in this letter. Two state-of-the-art techniques, DCO-OFDM and ACO-OFDM, are considered to obtain positive and real-valued OFDM symbols [9], [10]. In DCO-OFDM, $N/2-1$ symbols in $\mathbf{X}(n)$, $n=1,\cdots,N/2-1$, are put into the first half of subcarriers and the DC subcarrier (the first subcarrier) is set to zero. In ACO-OFDM, $N/4$ QAM symbols in $\mathbf{X}(n)$, $n=1,\cdots,N/4$, are mapped on to half of the odd subcarriers of the OFDM frame, $\mathbf{X}(k)$, $k=1,3,5,\cdots,N/2-1$. At the same time, the even subcarriers are set to zero. In both ACO-OFDM and DCO-OFDM, Hermitian symmetry is applied to the rest of the OFDM frame in order to obtain real-valued symbols through the IFFT block. Since LED transmitters can only send unipolar signals, the real-valued OFDM symbols need to be clipped. In DCO-OFDM, a DC bias is added to make the signal unipolar [10]. The DC bias, which is related to the average power of the OFDM symbols, is introduced and defined in [9] as,

$$B_{\mathrm{DC}}=\alpha\sqrt{\mathrm{E}\{\mathbf{x}^2(k)\}}, \tag{1}$$

where $\mathbf{x}(k)$ is the OFDM symbol frame vector, and $10\log_{10}(\alpha^2+1)$ is defined as the bias level in dB. The bias level in the current simulations is set to 7 dB and 13 dB, which are adopted from [9] for consistency. After the DC-bias, the OFDM frame is simply clipped by,

$$\mathbf{x}_{\mathrm{clipped}}(k)=\begin{cases}\mathbf{x}_{\mathrm{biased}}(k), & \mathbf{x}_{\mathrm{biased}}(k)\geq 0,\\ 0, & \mathbf{x}_{\mathrm{biased}}(k)<0,\end{cases} \tag{2}$$

where $\mathbf{x}_{\mathrm{biased}}(k)$ is the DC-biased symbol which is calculated as $\mathbf{x}_{\mathrm{biased}}(k)=\mathbf{x}(k)+B_{\mathrm{DC}}$. The clipped unipolar symbol is denoted by $\mathbf{x}_{\mathrm{clipped}}(k)$. In ACO-OFDM, since symbols are antisymmetric, clipped unipolar symbols are obtained by setting the negative part to zero. In the simulation, after being transformed into an optical intensity signal, the clipped signal is transmitted by a LED.

In this letter, we focus on the performance comparison between SPAD and PD over a long distance and in the absence of background light, and thus optical signals are assumed to pass through a flat fading channel and to be distorted by shot noise and/or thermal noise. The thermal noise is dominant in the case of PD receivers while the shot noise caused by the received signal and the detector's dark current are the major noise contributors in a SPAD receiver. Assuming that there is no other distortion effect during the transmission, the recovered signal, $\mathbf{x}'(k)$, can be scaled to the original clipped signal, $\mathbf{x}_{\mathrm{clipped}}(k)$. The recovered OFDM symbols from the SPAD or the PD are passed through a FFT operation. In DCO-OFDM, $N/2-1$ symbols are obtained from the corresponding subcarriers to constitute a QAM symbol frame, $\mathbf{X}'(n)$. In ACO-OFDM, $N/4$ symbols are obtained. The detected QAM symbols are then decoded by using an estimator in order to obtain the output bit stream.

B. SPAD Receiver

A SPAD device is an APD in the 'Geiger' mode which emits a very large current by receiving a single photon and thus can essentially be modelled as a single photon counter. The photodetection process of an ideal photon counter can be modelled using Poisson statistics which describe the shot noise effect ([11] and references therein).

In this letter, we consider an array of SPADs [12] which outputs the superposition of the photon counts from the individual SPADs. In order to generate received O-OFDM samples, the output of the SPAD array is counted over a short-time average period, T_{ST}, at time instances $t_k=kT_s$ of the received optical signal $\mathbf{x}_{\mathrm{r}}(t)$. These photon counts are denoted by $\nu(k)$ as shown in Fig. 1. Note that T_s which denotes the sampling period of the time-domain OFDM signal at the transmitter is assumed to be much larger than T_{ST}.

The photon detection rate of SPADs is typically limited by a number of practical constraints such as the SPAD dead time. In fact, each individual SPAD in the array can only receive one photon during the dead time, τ_{d}. Thus, the maximum number of counted photons in T_{ST} is,

$$\nu_{\max}\leqslant\frac{N_{\mathrm{SPAD}}T_{\mathrm{ST}}}{\tau_{\mathrm{d}}}, \tag{3}$$

where N_{SPAD} is the number of SPAD devices in the array. If the number of incoming photons is more than $\nu_{\max}$, the number of counted photons will be clipped which causes a receiving clipping distortion problem. In this letter, however, we assume that the short-time average period, T_{ST}, is much longer than the dead time. Thus the photon counts at the output

TABLE I
SIMULATION PARAMETERS

The wavelength of the received light λ_{L}	450 nm
The PDE of the SPAD C_{PDE} [12]	20%
The DCR of the SPAD N_{DCR} [12]	7.27 kHz
The dead time of the SPAD τ_{d} [12]	13.5 ns
Number of SPADs in an array N_{SPAD} [12]	1024
The responsivity of the PD	0.2
Input referred noise of the PD	16 pA/$\sqrt{\mathrm{Hz}}$

of the SPAD array (i.e., $\nu(k)$) can be still described by Poisson distribution as,

$$\Pr(\nu(k) = j) = \exp(-\mu(k))\frac{\mu(k)^{-j}}{j!}, \tag{4}$$

where the average photon counts $\mu(k)$ can be expressed as a function of the received signal and the SPAD's dark count rate (DCR), N_{DCR}, as,

$$\mu(k) = \frac{C_{\mathrm{PDE}}}{E_{\mathrm{P}}}\int_{t_k}^{t_k+T_{\mathrm{ST}}} \mathbf{x}_{\mathrm{r}}(t)\mathrm{d}t + N_{\mathrm{DCR}}T_{\mathrm{ST}}, \tag{5}$$

where C_{PDE} denotes the photon detection efficiency (PDE) of the SPADs. Note that the shot noise described above is not only caused by the randomness in receiving discrete signal photons but also generated by the SPAD's dark photon emission at the fixed rate N_{DCR}. The energy of a photon is E_{P} which is calculated by $\frac{hc_{\mathrm{L}}}{\lambda_{\mathrm{L}}}$. Planck's constant is represented by h; c_{L} is the speed of the light; and λ_{L} is the wavelength of the light.

The output of the SPAD array is the number of photons, and the system is designed for an O-OFDM demodulator which requires the amplitude of the electrical signal (optical power) to demodulate the received signal to the original encoded bits. Thus, the photon-to-amplitude equalizer is used to simply convert the received photon number to the corresponding electrical signal amplitude (optical power), $\mathbf{x}'(k)$. The coefficient of the equalizer is calculated by a pilot which captures the effect of channel attenuation and PDE.

III. RESULTS AND COMPARISONS

The performance of an OFDM system employing either a SPAD receiver as described in Section II or a standard PD receiver as used in [9] is investigated. The LED transmitter emits blue light with a wavelength distribution centered around 450 nm. We consider a SPAD array of size $N_{\mathrm{SPAD}} = 1024$ as introduced in [12]. In the PD-based OFDM system, a high speed PIN receiver, New Focus 1601FS-AC, is used. The PD receiver has been used and tested in [1]. Since there is no background light, the thermal noise is the main noise component at the PD receiver. The parameters which are applied in the simulation are given in Table I.

A. Performance of OFDM With SPAD

Fig. 2 shows the simulation results for the BER of the SPAD-based DCO-OFDM system as a function of the optical irradiance when the transmission speed is 1 kbits/s.

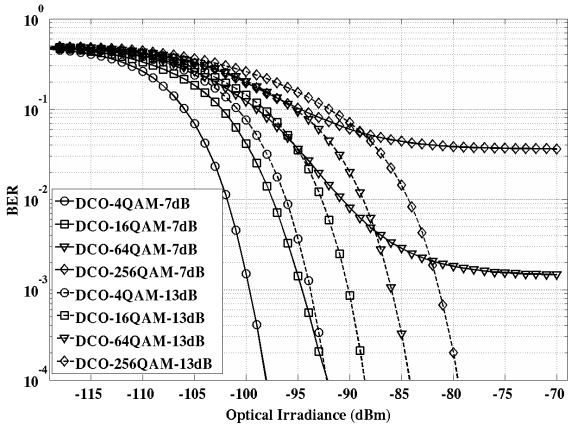

Fig. 2. The bit error ration (BER) performance of the SPAD-based DCO-OFDM system, for the transmission speed of 1 kbits/s.

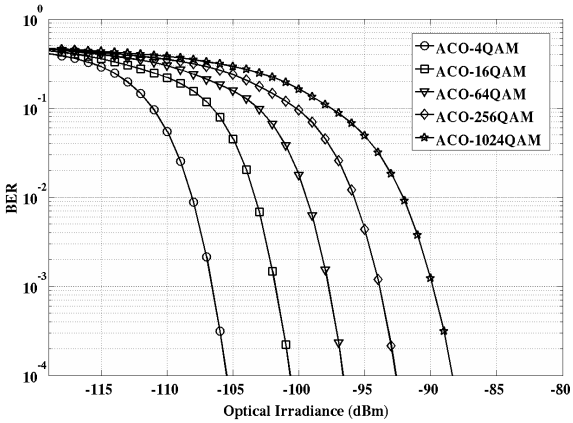

Fig. 3. The BER performance of the SPAD-based ACO-OFDM system, for the transmission speed of 1 kbits/s.

The performance of DCO-OFDM for 4, 16, 64 and 256-QAM with 7 dB and 13 dB DC-bias are compared in this figure. For DCO-OFDM with lower constellation sizes (4, 16-QAM), the 7 dB DC-bias system requires less optical irradiance than the 13 dB system. For 64-QAM and 256-QAM, clipping distortions create an error floor in DCO-OFDM with 7 dB DC-bias. Thus for higher constellation sizes, a higher DC-bias may need to be applied in DCO-OFDM.

Fig. 3 shows the BER performance of the SPAD-based ACO-OFDM system. The transmission speed is also set to 1 kbits/s. Modulation schemes are 4, 16, 64, 256 and 1024-QAM. Compared with DCO-OFDM, ACO-OFDM requires less energy as expected. As shown in Fig. 3, the 4-QAM SPAD-based ACO-OFDM system is able to demodulate the signal by receiving only -107 dBm optical power to at a BER of 10^{-3}. For 4-QAM DCO-OFDM with 7 dB DC-bias, the optical power required at the SPAD receiver is approximately -100 dBm. The higher power efficiency of ACO-OFDM comes at the expense of approximately half spectral efficiency.

B. Comparison Between SPAD and PD

Fig. 4 and Fig. 5 show the simulation results of the performance comparison between the SPAD-based OFDM

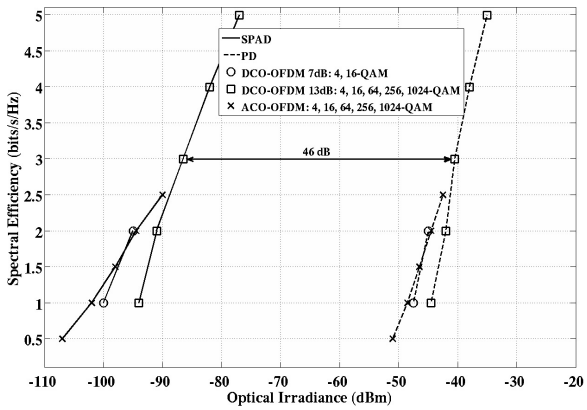

Fig. 4. Spectral efficiencies for a BER of 10^{-3} and transmission speed of 1 kbits/s versus optical irradiance.

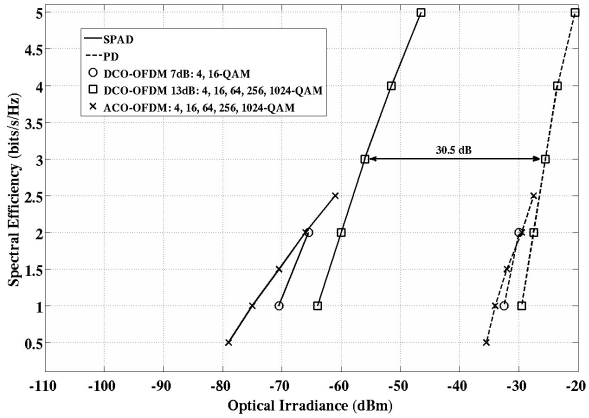

Fig. 5. Spectral efficiencies for a BER of 10^{-3} and transmission speed of 1 Mbits/s versus optical irradiance.

system and the PD-based OFDM system. The figures show the spectral efficiency of ACO-OFDM and DCO-OFDM with 7 dB and 13 dB bias versus optical irradiance, for a BER of 10^{-3} and transmission speed of 1 kbits/s and 1 Mbits/s, respectively. Both figures show that the SPAD-based OFDM system needs much less optical irradiance than the PD-based OFDM system. A SPAD triggers billions of electron-hole pairs by a single detected photon. As a consequence, the SPAD-based OFDM system can demodulate signals from a relatively lower number of photons, and consequently exhibits a much higher receiver sensitivity. The PD-based OFDM system needs more power to offset the effect of the thermal noise at the amplifier. For example, in Fig. 4, the SPAD-based OFDM system with 13 dB bias needs 46 dB less optical irradiance than the PD-based OFDM system with 13 dB bias at 3 bits/s/Hz. When compared with 1 kbits/s transmission speed (Fig. 4), for 1 Mbits/s (Fig. 5), the SPAD system has 30.5 dB greater power efficiency than the PD system. In Fig. 5, by significantly increasing the data rate, the number of photon counts at each sample drops with the same rate (1000 times) over the whole SPAD array resulting in a very low signal-to-error count ratio. Therefore, the received optical power needs to be significantly increased to ensure a reliable BER performance. When using the PD receiver, the required received optical power increases also as the data rate is augmented, but there is no energy loss due to detector dead times which is particularly critical when the dead time is approaching the sampling time. Therefore, the increasing data rate affects the error performance less significantly compared to the SPAD receiver.

IV. Conclusion

In this letter, an O-OFDM system with a SPAD receiver is presented and compared with state-of-the-art PD-receiver based O-OFDM systems. When the transmission power and speed are low, in the region of 1 kbit/s, the SPAD-based OFDM system has significantly better performance than the PD-based OFDM system. However, when the transmission speed is 1 Mbits/s, the SPAD-based DCO-OFDM system with 13 dB DC bias still enhances the sensitivity by a staggering 30.5 dB over the PD-based DCO-OFDM system. The higher receiver sensitivity means that the SPAD-based OFDM system can be used in long distance transmissions, or in non-line of sight optical wireless communications, in the uplink when illumination is not essential, or when lights are almost completely dimmed. Note, the reported sensitivities are in the range of those known from standard RF systems.

References

[1] D. Tsonev *et al.*, "A 3-Gb/s single-LED OFDM-based wireless VLC link using a gallium nitride μLED," *IEEE Photon. Technol. Lett.*, vol. 26, no. 7, pp. 637–640, Apr. 1, 2014.

[2] J. M. Kahn and J. R. Barry, "Wireless infrared communications," *Proc. IEEE*, vol. 85, no. 2, pp. 265–298, Feb. 1997.

[3] J. Armstrong, "OFDM for optical communications," *J. Lightw. Technol.*, vol. 27, no. 3, pp. 189–204, Feb. 1, 2009.

[4] D. Tsonev, S. Sinanović, and H. Haas, "Novel unipolar orthogonal frequency division multiplexing (U-OFDM) for optical wireless," in *Proc. IEEE 75th Veh. Technol. Conf. (VTC Spring)*, May 2012, pp. 1–5.

[5] Y. Li, D. Tsonev, and H. Haas, "Non-DC-biased OFDM with optical spatial modulation," in *Proc. IEEE 24th Int. Symp. Pers. Indoor Mobile Radio Commun. (PIMRC)*, Sep. 2013, pp. 486–490.

[6] D. Tsonev and H. Haas, "Avoiding spectral efficiency loss in unipolar OFDM for optical wireless communication," in *Proc. IEEE Int. Conf. Commun. (ICC)*, Jun. 2014, pp. 3336–3341.

[7] Y. Li, S. Videv, M. Abdallah, K. Qaraqe, M. Uysal, and H. Haas, "Single photon avalanche diode (SPAD) VLC system and application to down-hole monitoring," in *Proc. IEEE Global Commun. Conf. (GLOBECOM)*, Austin, TX, USA, Dec. 2014, pp. 2108–2113.

[8] D. Chitnis and S. Collins, "A SPAD-based photon detecting system for optical communications," *J. Lightw. Technol.*, vol. 32, no. 10, pp. 2028–2034, May 15, 2014.

[9] J. Armstrong and B. Schmidt, "Comparison of asymmetrically clipped optical OFDM and DC-biased optical OFDM in AWGN," *IEEE Commun. Lett.*, vol. 12, no. 5, pp. 343–345, May 2008.

[10] S. Dimitrov, S. Sinanovic, and H. Haas, "Clipping noise in OFDM-based optical wireless communication systems," *IEEE Trans. Commun.*, vol. 60, no. 4, pp. 1072–1081, Apr. 2012.

[11] M. Safari, M. M. Rad, and M. Uysal, "Multi-hop relaying over the atmospheric Poisson channel: Outage analysis and optimization," *IEEE Trans. Commun.*, vol. 60, no. 3, pp. 817–829, Mar. 2012.

[12] E. Fisher, I. Underwood, and R. Henderson, "A reconfigurable single-photon-counting integrating receiver for optical communications," *IEEE J. Solid-State Circuits*, vol. 48, no. 7, pp. 1638–1650, Jul. 2013.